Correction

For the article "Neuronal Transporters Regulate Glutamate Clearance, NMDA Receptor Activation, and Synaptic Plasticity in the Hippocampus" by Annalisa Scimemi, Hua Tian, and Jeffrey S. Diamond, which appeared on pages 14581–14595 of the November 18, 2009 issue, the authors have issued the following correction.

Through recent correspondence with Drs. Robert Thorne and Charles Nicholson, we have come to realize that in our paper (Scimemi et al., 2009), we had erroneously calculated the hydrodynamic diameter (d_H) of the fluorescent probes used for the integrative optical imaging (IOI) results (Fig. 3*B*,*C*, Table 1). We inadvertently used the effective diffusion coefficient (D^*), instead of free diffusion coefficient (D_{free}), in determining d_H from the Stokes–Einstein equation. The correct values of d_H, together with new estimates of D_{free} for all fluorescent probes used in IOI, are now listed in the new version of Table 1 and Figure 3. This correction does not affect one of the major conclusions of the paper—that the diffusion properties of the hippocampal neuropil in wild-type and EAAC1 KO mice are similar.

The values of D_{free} we initially reported were 1.4- to 4.6-fold higher than those previously obtained for similar probes in various brain tissues using IOI and other approaches including dynamic light scattering (Shao and Baltus, 2000), intrinsic viscosity measurements (Armstrong et al., 2004), and fluorescence recovery after photobleaching (Pluen et al., 1999; Syková and Nicholson, 2008). The primary methodological difference between our D_{free} measurements and those obtained by Thorne and Nicholson (2006), both with IOI, is that ours were performed in free solution, whereas those of Thorne and Nicholson (2006) were obtained in 0.3% agarose (w/v). We have repeated our measurements of D_{free} in free solution, and obtained similar results to those we presented in our original manuscript. Additional IOI measurements of the diffusion coefficient of our dyes (D') in various agarose concentrations (Cat. A9045 Sigma; 0.1, 0.2, and 0.3% w/v) enabled us to obtain values of D_{free} smaller than those derived in free solution and similar to those reported by Syková and Nicholson (2008). We conclude that the values of D_{free} we reported previously were likely confounded by the hydrodynamic flow created by the puff application in free solution. We have used these new values and expanded our measures of D^* for QD655 in WT and KO slices to recalculate $\lambda_{\theta=0}$ and ECS width with the parallel plane geometry approximation (Fig. 3*C*). The new values are $\lambda_{\theta=0} = 1.25 \pm 0.09$ and ECS $= 52.24 \pm 0.64$ nm in WT and $\lambda_{\theta=0} = 1.18 \pm 0.08$ and ECS $= 51.44 \pm 0.45$ nm in EAAC1 KO, consistent with those obtained with 2P-LSM (Fig. 3*E*). The reasons for the discrepancy between our new values of d_H and λ (corrected version of Table 1) and those reported by Syková and Nicholson (2008) remain unclear, but the similarity between λ and ECS width in WT and KO slices still confirm that diffusion of small molecules is similar in WT and EAAC1 KO slices.

In synthesis, we provide a revised analysis for our IOI measures of D_{free}, d_H, D^*, λ, $\lambda_{\theta=0}$, and ECS. This analysis still confirms a major conclusion of the paper—that the structural and diffusion properties of the hippocampal neuropil are not altered by genetic deletion of EAAC1. We thank Drs. Thorne and Nicholson for their comments on our manuscript and for their help with this revision.

A corrected and expanded section of the supplemental material is published below.

Diffusion measurements using integrative optical imaging

We used previously described methods (Thorne and Nicholson, 2006) to image the diffusion of Texas red dextrans (3, 10, 40, and 70 kDa; TRdx3, TRdx10, TRdx40, and TRdx70, respectively) and red-fluorescent quantum dot nanocrystals (Qtracker 655 nontargeted quantum dots, QD655). All fluorescent molecules were purchased from Invitrogen. TRdx3 (Cat. D3329) and TRdx10 (Cat. D1828) were used at a concentration of 1 mM, whereas TRdx40 (Cat. D1829) and TRdx70 (Cat. D1830) were used at a concentration of 0.1 mM. QD655 (Cat. Q21021MP) was used at the concentration formulated by the manufacturer (2 μM in 50 mM borate buffer, pH 8.3). Agarose was purchased from Sigma (Cat. A9045). Each fluorescent probe was pressure applied (200 ms × 5–7 PSI) in three different agarose solutions (0.1, 0.2, and 0.3%, w/v) prepared in distilled water or ACSF (no difference was observed and data were pooled) kept at room temperature (24°C) for at least 1 h, and in stratum radiatum of WT and KO hippocampal slices using a glass pipette [1.5–2.5 MΩ; 30-0057 (GC150F-10), Warner Instruments] connected to a Picospritzer III (Parker Hannifin Corporation General Valve Division). An area of 720 × 540 μm was imaged using a Zeiss Achroplan 10X water-immersion objective (0.5 NA) with a 0.8 magnification. Illumination was provided by a 100 W halogen epifluorescence lamp (AttoArc HBO, Zeiss), controlled by a Uniblitz shutter and driver or by a 530 nm, 10 mW LED (OptoLed Light Source, Cairn Research). No difference in D or D^* was observed when using these illumination systems, and data were pooled. Images were recorded with a CCD camera (N50, Hamamatsu Photonics; 640 × 480 pixels), and acquired with a Scion FG-7 frame grabber (Scion). For diffusion measures in agarose solutions, we acquired one frame every second, for 30 s. For diffusion measures in hippocampal slices, we acquired one frame every 1–5 s for 1–10 min, depending on the dye. The projection of the 3D cloud of diffusing probe on the 2D image plane of the camera was described by the following:

$$I_i(r, \gamma_i) = A_i e^{-\left(\frac{r}{\gamma_i}\right)^2}$$

and

$$\gamma_i^2 = 4D^*(t_i + t_0),$$

where I_i = fluorescence intensity of the ith image at radial distance r from the source, A_i = an expression that incorporates the defocused point spread function of the microscope, and t_0 = time offset from the time of the puff application t_i. The first expression was used to fit the concentration distributions at time $t_1, t_2 \ldots t_n$ (Levenberg–Marquardt algorithm, IgorPro) to derive γ_i (the width of the Gaussian function at time $t_1, t_2 \ldots t_n$). The signal of the background image was subtracted from that of the images taken after the puff. The concentration distributions we obtained displayed radial symmetry and a Gaussian profile. They were analyzed only on a plane

Table 1. Summary of the diffusion parameters estimated through the integrative optical imaging approach in free solution and in WT and KO slices

			D^* (μm^2/ms)		λ	
Probe	D_{free} (μm^2/ms)	d_H (nm)	WT	KO	WT	KO
TRdx3	0.160 ± 0.077 (6)	5.11 ± 3.39	0.103 ± 0.023 (11)	0.112 ± 0.031 (9)	1.27 ± 0.14	1.22 ± 0.17
TRdx10	0.118 ± 0.027 (6)	5.39 ± 1.12	0.074 ± 0.010 (8)	0.076 ± 0.010 (8)	1.11 ± 0.07	1.10 ± 0.07
TRdx40	0.064 ± 0.022 (6)	10.80 ± 4.20	0.016 ± 0.003 (10)	0.017 ± 0.004 (8)	1.77 ± 0.14	1.75 ± 0.22
TRdx70	0.037 ± 0.009 (6)	17.64 ± 5.23	0.013 ± 0.014 (14)	0.012 ± 0.001 (12)	1.99 ± 0.47	1.77 ± 0.10
QD655	0.016 ± 0.009 (6)	48.64 ± 23.67	0.0004 ± 0.0002 (8)	0.0007 ± 0.0007 (7)	7.14 ± 3.49	7.56 ± 4.33

Data are presented as mean ± SD. The numbers in parentheses represent the number of experiments done. All experiments were performed on multiple slices from multiple animals. All dyes were purchased from Sigma (TRdx3 1 mM Cat. D3329; TRdx10 1 mM Cat. D1828; TRdx40 0.1 mM Cat. D1829; TRdx70 0.1 mM Cat. D1830; QD655 2 μM Cat. Q21021MP). The D_{free} measures were performed by puffing each fluorescent probe in three different solutions of agarose purchased from Sigma (Cat. A9045) (0.1, 0.2, and 0.3%, w/v) prepared in distilled water or ACSF (no difference was observed and data were pooled) kept at room temperature (24°C) for at least 1 h. These values were corrected for $Q_{10} = 1.3$ and represent the values of D_{free} at 34 °C. The reported values of d_H and λ represent the average of individual measures.

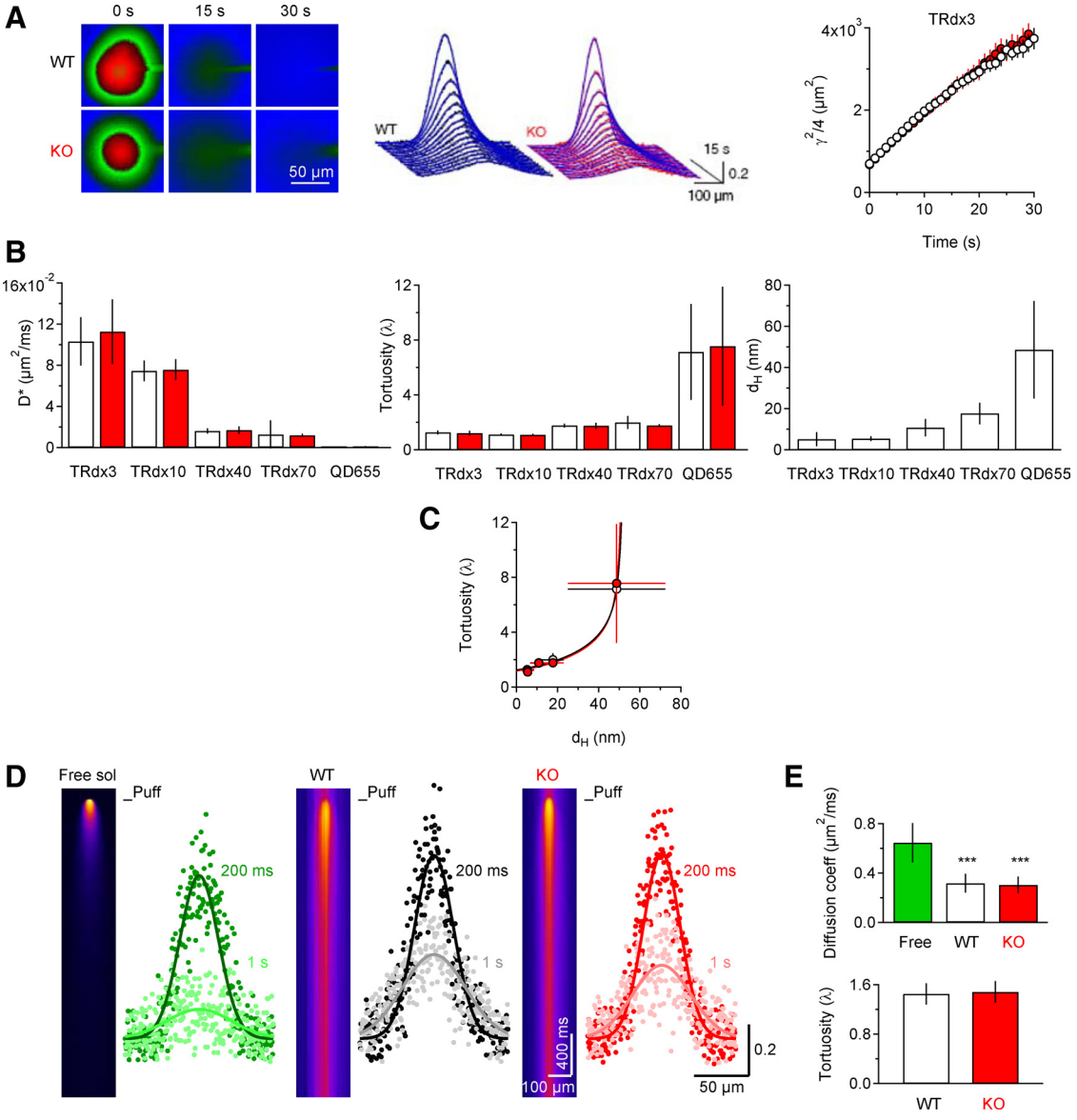

Figure 3. Diffusion in the hippocampal neuropil is similar in WT and KO mice. ***A***, Representative images of TRdx3 diffusion in stratum radiatum of WT (top) and KO (bottom) mice. Middle, Fluorescence intensity profiles and theoretical fits for these images. Right, A linear regression of $\gamma^2/4$ over time yields an estimate of D^* for TRdx3. ***B***, Summary of the effective diffusion coefficient (D^*) and tortuosity (λ) in WT and KO neuropil and of the hydrodynamic diameter (d_H) for various fluorescent probes at 34°C (D^* TRdx3 WT $n = 11$, KO $n = 9$, $p = 0.44$, Power = 0.17; TRdx10 WT $n = 8$, KO $n = 8$, $p = 0.81$, Power = 0.10; TRdx40 WT $n = 10$, KO $n = 8$, $p = 0.60$, Power = 0.14; TRdx70 WT $n = 14$, KO $n = 12$, $p = 0.84$, Power = 0.08; QD655 WT $n = 8$, KO $n = 7$ $p = 0.46$, Power = 0.28) (λ TRdx3 $p = 0.53$, Power = 0.17; TRdx10 $p = 0.80$, Power = 0.08; TRdx40 $p = 0.76$, Power = 0.08; TRdx70 $p = 0.13$, Power = 0.33; QD655 $p = 0.84$, Power = 0.07). The numerical values are presented in Table 1. ***C***, By using a model of parallel plane geometry for the hippocampal neuropil (Thorne and Nicholson, 2006), we show a similar diffusion behavior of the Texas red probes in WT and KO slices. The predicted values of $\lambda_{\theta=0}$ (the estimated tortuosity for a vanishingly small molecule) are $\lambda = 1.25 \pm 0.09$ (WT) and $\lambda = 1.18 \pm 0.08$ (KO). The estimated ECS width is 52.24 ± 0.64 nm (WT) and 51.44 ± 0.45 nm (KO). ***D***, Fluorescence intensity profiles for AlexaFluor 350 pressure applied in free medium (left), WT (middle), or KO slices (right). Each image represents the average of 10 consecutive trials, and the intensity profiles are measured 200 ms and 1 s after the puff. ***E***, Summary of the diffusion coefficient and tortuosity measured in each condition at room temperature (top: D_{free} 0.64 ± 0.16 μm^2/ms, $n = 6$; D^*_{WT} 0.32 ± 0.08 μm^2/ms, $n = 8$; D^*_{KO} 0.30 ± 0.07 μm^2/ms, $n = 9$, $D_{free} - D^*_{WT}$ ***$p = 0.0002$, $D_{free} - D^*_{KO}$ ***$p = 6.1 \times 10^{-5}$, $D^*_{WT} - D^*_{KO} p = 0.68$, Power = 0.13; bottom: λ_{WT} 1.45 ± 0.17; λ_{KO} 1.48 ± 0.17, $p = 0.71$, Power = 0.09). The estimated values of the diffusion coefficients at 34°C, obtained by multiplying the previous values by $Q_{10} = 1.3$, are as follows: D_{free} 0.84 ± 0.21 μm^2/ms; D^*_{WT} 0.41 ± 0.10 μm^2/ms; D^*_{KO} 0.39 ± 0.09 μm^2/ms.

orthogonal to the direction of the puff, to minimize any potential artifact due to puff applications of different fluorescent probes. The free and effective diffusion coefficients were estimated from the linear regression of $\gamma^2/4$ versus t_i. The values of D_{free} and D^* in Table 1 refer to the free and effective diffusion coefficients of various probes at 34°C, respectively.

The tortuosity value of each probe (λ) was measured as follows:

$$\lambda = \sqrt{\left(\frac{D}{D^*}\right)}.$$

The hydrodynamic diameter of different molecules (d_H) was calculated from the Stokes–Einstein equation:

$$d_H = \frac{KT}{3\pi\eta D},$$

where K = Boltzmann's constant ($1.38 \cdot 10^{-23}$ J/K), T = temperature in kelvins (307), η = viscosity of water at 307 K ($7.35 \cdot 10^{-4}$ Pa · s) and $D = D_{free}$, the estimated diffusion coefficient of each probe in free solution at 307 K. We monitored diffusion of all fluorescent probes in 0.1, 0.2, and 0.3% agarose solutions. Diffusion tended to be faster in lower agarose gels, but no significant difference was observed in different agarose solutions, so data were pooled. These values of D_{free} are listed in the new version of Table 1. We also measured extrapolated D_{free} for a solution with the same viscosity of water, from a plot of D versus the viscosity of each agarose solution, for all our probes. The kinematic viscosity (η) of water and of 0.1–0.3% agarose solutions at 24°C was measured using a glass capillary viscometer (Cannon Instrument), and values were adjusted by $Q_{10} = 1.3$ to account for the temperature dependence of diffusion and derive the value of D_{free} at 34°C.

To calculate the average width of the ECS (d_{ECS}), we assumed a parallel plane geometry (Thorne and Nicholson, 2006) and fitted our results with the following equation:

$$\lambda = \lambda_{\theta=0}[(1-\theta)(1-1.004\theta+0.418\theta^3+0.21\theta^4-0.169\theta^5)]^{-\frac{1}{2}},$$

where $\lambda_{\theta=0}$ is λ for a vanishingly small molecule and $\theta = d_H/d_{ECS}$ (Thorne and Nicholson, 2006).

All data in the updated figure and table are presented as mean ± SD. The numbers in parentheses represent the number of experiments done. All experiments were performed on multiple slices from multiple animals.

References

Armstrong JK, Wenby RB, Meiselman HJ, Fisher TC (2004) The hydrodynamic radii of macromolecules and their effect on red blood cell aggregation. Biophys J 87:4259–4270.

Pluen A, Netti PA, Jain RK, Berk DA (1999) Diffusion of macromolecules in agarose gels: comparison of linear and globular configurations. Biophys J 77:542–552.

Scimemi A, Tian H, Diamond JS (2009) Neuronal transporters regulate glutamate clearance, NMDA receptor activation, and synaptic plasticity in the hippocampus. J Neurosci 29:14581–14595.

Shao J, Baltus RE (2000) Hindered diffusion of dextran and polyethylene glycol in porous membranes. AICHE J 46:1149–1156.

Syková E, Nicholson C (2008) Diffusion in brain extracellular space. Physiol Rev 88:1277–1340.

Thorne RG, Nicholson C (2006) In vivo diffusion analysis with quantum dots and dextrans predicts the width of brain extracellular space. Proc Natl Acad Sci U S A 103:5567–5572.